# IAM Assignment 2 - Investigating flocking mechanisms in birds through modelling

**David Batchelder**

**Figure 1.** A flock of Starlings next to Brighton Pier, January 2023[1]

## Introduction

Throughout our world we frequently witness emergent properties, such as collective motion, that arise from the interaction of a set of individuals. This phenomenon is found in systems constituted both by living and non-living individuals. Examples emphasizing this ubiquity include fish schools[2,3], macromolecules[4], financial markets[5], and traffic flows[6]. Bird flocks are a particularly pertinent demonstration of collective motion with species such as the European Starling producing striking displays of flocking - typically referred to as murmurations. Likely explanations for the existence of flocking behaviour come from evolutionary advantage - birds in a flock can better detect predators[7], as well as benefiting from foraging as a group[8]. Therefore, the formation and maintenance of a robustly cohesive flock (one that can maintain structure even after perturbations, e.g. a predator attack) is of utmost importance to the survival of these species.

Since the seminal work of Reynolds[9] a large amount of study has been devoted to analysis of computational models designed to simulate these systems. A large proportion of these are agent-based models that typically employ three forces (or a subset of them) that repulse, align, and attract agents within certain ranges. Determining the mechanisms that species such as the European Starling use to maintain cohesion is a particularly challenging problem due to the nature of emergent properties - one cannot simply analyse the individuals, but instead must look at the collective. Another historical obstacle was the lack of experimental data of large flocks - making it hard to validate computational models. With the advancement of technology this is now starting to be less of a problem. Work such as Ballerini et al[10], which produced the first large scale 3D positional data of up to 2,600 European Starlings, has uncovered crucial insights which will enable a new level of understanding of collective motion in this species, as well as contributing to our general understanding of collective motion. It is the work of Ballerini et al[10] on which I base my report.

Much of the previous work in this field has held the assumption that metric distance is the measure used to dictate interaction with other agents. For example, Couzin et al[11] introduced an agent-based model for flocking in three dimensions to analyse spatial dynamics of bird flocks and fish schools. This was based on the standard repulsion, orientation, and attraction forces, where each force was applied to one of three non-overlapping metric ranges - essentially each bird had constant spherical regions around it which would determine its interactions. This model (along with many other models within the field[12,13,14]) can produce dynamics which are seen in nature such as swarming and dynamic parallel motion (See Couzin et al[11] for definition of dynamics), typical behaviour respectively seen in mosquitoes and flocking birds. However, the findings of Ballerini et al[10] appear to contradict the assumption of metric distance determining interactions. By analysing the spatial distribution of nearest neighbours within the recorded flocks, they were able to show the existence of structure in the spatial distribution of up to 6-7 nearest neighbours - with no structure present for further neighbours, which implies they are non-interacting. The crucial fact is that this same pattern was seen in flocks with varying densities. Further analysis of correlations under the metric and

topological cases produced evidence that "the structure, and thus indirectly the interaction causing it, depends on the topological distance rather than the metric distance" (Ballerini et al[10]).

While this result does incite the revision of previous models to include topological considerations (Several works have already implemented updated models[12 ,15]), it does not indicate the local interaction mechanisms that are employed by the species. This is an issue that I will attempt to shine a light on in this report through the analysis of biologically motivated computational models. Ballerini et al[10] implemented an elementary model based on Vicsek et al[16] to demonstrate the benefits of topological interactions with regards to robust cohesiveness. This 2D model is useful in highlighting this point due to its simplicity, but this simplicity is also a limitation in terms of hypothesis testing in more biologically plausible conditions. Here I base my analysis on the work of Ballerini et al[10] but implement an extended model which works in three dimensions and incorporates more realistic movement and perceptual abilities. Using this model I will replicate the analysis of cohesion of the flock under simulated predator attacks as in[10]. This extension will allow for comparison of simulated and experimental data to aid in deduction of individual rules that European Starlings (with potential to be used similarly for other species and animals such as fish) use to produce collective motion. Couzin et al[11] provide a simple and well analysed model which I will use as a foundation and for comparison - similarly to the work of Mudaliar et al[12]. This model has features such as a limited field of view and limited turning rate which enables experimentation under more realistic conditions.

## Methods

### Model

Couzin et al[11] proposed a three-dimensional agent-based model based on the standard three forces of repulsion, orientation, and attraction. They implement each of these forces over metric ranges, whereas my model uses topological distance-based ruling following the work of Ballerini et al[10]. I also introduce a combined metric and topological distance-based model to investigate and discuss its natural plausibility. This model does not suffer from a lack of cohesion for low number of interactions, as the metric and topological model are known to. Below I provide a formulation of the topological model as in Mudaliar et al[12], but each of these models follow this format, except the sets R, O, and A are calculated according to the distance type.

#### *Notation*

Using similar notation to previous work I assign the position of N individuals ($i = 1,2,...,N$) at the discrete time period $t$ as $\boldsymbol{c}_i(t)$ with velocity $\boldsymbol{v}_i(t) = u_i(t)\boldsymbol{i} + v_i(t)\boldsymbol{j} + w_i(t)\boldsymbol{k}$, and associated unit direction vector $\hat{\boldsymbol{v}}_i(t) = \hat{u}_i(t)\boldsymbol{i} + \hat{v}_i(t)\boldsymbol{j} + \hat{w}_i(t)\boldsymbol{k}$ where $\boldsymbol{i}$, $\boldsymbol{j}$, and $\boldsymbol{k}$ are the unit vectors at the origin which point along the $x$, $y$, and $z$ axis respectively. Time steps are separated equally by time $\Delta t$. At each time step an updated direction vector $\boldsymbol{d}_i(t+\Delta t)$ is calculated for each individual, positions are updated synchronously. Individuals are repulsed from one another if they are within $r_r$ distance of one another. Individuals all move at a constant speed of $s$, and have a field of view limited by a blind zone at their rear - the angle of which is denoted $\omega_{blind}$. The blind zone does not apply to birds within the zone of repulsion which follows earlier work[11 ,17] - a natural explanation is that a bird is likely to sense another bird this close through one of its other senses. Noise is introduced into the model by applying a random perturbation to the direction vector $\boldsymbol{d}_i(t+\Delta t)$ - the amount of noise is controlled by a parameter $\eta$. Each bird is limited to a turning angle of $\theta_{\Delta t}$ at each time step. $n_o$ and $n_a$ respectively denote the number of individuals we consider for the orientation and attraction interactions in the topological model.

#### *Behavioural rules*

An individual first detects if there are any other individuals within its repulsion zone - R denotes the set of individuals in this zone. If R is non-empty, the individual will adjust its direction to move away from these individuals according to the formula below:

$$\boldsymbol{d}_{r_i}(t+\Delta t) = -\sum_{j \in R} \frac{r_{ij}(t)}{|r_{ij}(t)|}$$

where $r_{ij} = c_j - c_i$, the vector from individual i to j. If R is non-zero then the direction in the next time step will solely be dictated by the repulsion interactions, avoiding collision takes priority. We normalise this direction vector to give $\hat{\boldsymbol{d}}_{r_i}(t+\Delta t) = \frac{\boldsymbol{d}_{r_i}(t+\Delta t)}{|\boldsymbol{d}_{r_i}(t+\Delta t)|}$.

If R is empty, we then consider the nearest neighbours and the orientation and attraction effects. Here we use topological distances to determine the nearest $n_o$ neighbours outside the repulsion zone, this set is denoted O. The individual will orient their velocity with these individuals according to the formula:

$$\boldsymbol{d}_{o_i}(t+\Delta t) = \sum_{j \in O} \frac{v_j(t)}{|v_j(t)|}$$

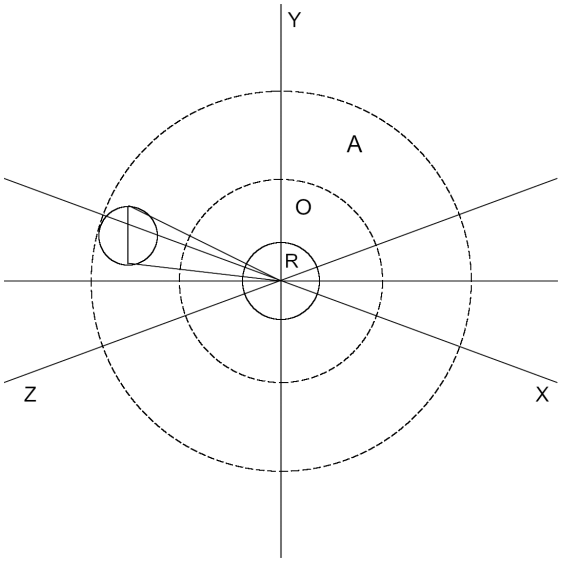


**Figure 2.** Visual representation of an individual centred at the origin. R is the fixed metric repulsion range, O is the orientation range which is variable depending on the topological range and the positioning of nearest neighbours, and A is the attraction range which varies according to the orientation topological range and position of nearest neighbours. The individual has a field of view of 360 - $\omega_{blind}$, the blind area can be seen as the cone that would be at the rear of a bird flying along the x-axis.

Finally, we consider the $n_a$ nearest neighbours after the $n_o$ nearest neighbour, this set is denoted by A. These individuals will apply an attractive force:

$$\boldsymbol{d}_{a_i}(t+\Delta t) = \sum_{j \in A} \frac{r_{ij}(t)}{|r_{ij}(t)|}$$

As with repulsion, we normalise these direction vectors: $\hat{\boldsymbol{d}}_{o_i}(t+\Delta t) = \frac{\boldsymbol{d}_{o_i}(t+\Delta t)}{|\boldsymbol{d}_{o_i}(t+\Delta t)|}$, $\hat{\boldsymbol{d}}_{a_i}(t+\Delta t) = \frac{\boldsymbol{d}_{a_i}(t+\Delta t)}{|\boldsymbol{d}_{a_i}(t+\Delta t)|}$.

The direction vector at the next step is then calculated according to the following cases (|X| denotes the cardinality of set X):

- Case 1: |R| > 0

$$\boldsymbol{d}_i(t+\Delta t) = \hat{\boldsymbol{d}}_{r_i}(t+\Delta t)$$

- Case 2: |R| = 0, |O| > 0, |A| = 0

$$\boldsymbol{d}_i(t+\Delta t) = \hat{\boldsymbol{d}}_{o_i}(t+\Delta t)$$

- Case 3: |R| = 0, |O| = 0, |A| > 0

$$\boldsymbol{d}_i(t+\Delta t) = \hat{\boldsymbol{d}}_{a_i}(t+\Delta t)$$

- Case 4: |R| = 0, |O| > 0, |A| > 0

$$\boldsymbol{d}_i(t+\Delta t) = \frac{1}{2}(\hat{\boldsymbol{d}}_{o_i}(t+\Delta t) + \hat{\boldsymbol{d}}_{a_i}(t+\Delta t))$$

Every case must result in a unit direction vector, hence we take

$$\hat{\boldsymbol{d}}_i(t+\Delta t) = \frac{\boldsymbol{d}_i(t+\Delta t)}{|\boldsymbol{d}_i(t+\Delta t)|} = \hat{d}_{x_i}(t+\Delta t)\boldsymbol{i} + \hat{d}_{y_i}(t+\Delta t)\boldsymbol{j} + \hat{d}_{z_i}(t+\Delta t)\boldsymbol{k}$$

.

### *Noise Input*

Analogous to Couzin et al[11] but in the 3D case, I apply a random perturbation to $\hat{\boldsymbol{d}}_i(t+\Delta t)$ following the implementation used in Mudaliar et al[12]. Mudaliar et al propose an approximation of spherically wrapped Gaussian random variates which is said to be suitably accurate for small standard deviations - this suits as we do not want large amounts of noise as this would destroy the interaction effects.

Using spherical coordinates, $\alpha$ is the angle of rotation from the $x$-axis in the horizontal $xy$-plane. $\psi$ is the colatitude, relative to the $z$-axis. Three random points about $(0,0,1)$ on the unit sphere are generated by the following random variates: $\tilde{\alpha}$ drawn

from a uniform distribution on $(0, 2\pi)$, and $\tilde{\psi}$ which is the absolute value of a normally distributed random variate with standard deviation $\eta$.

The cartesian coordinates of this randomly generated point on a unit sphere are:

$$(\tilde{x}, \tilde{y}, \tilde{z}) = (\cos\tilde{\alpha}\sin\tilde{\psi}, \sin\tilde{\alpha}\sin\tilde{\psi}, \cos\tilde{\psi})$$

To apply this noise, express $\hat{\boldsymbol{d}}_i(t+\Delta t)$ in spherical coordinates with azimuthal angle $\alpha_0$ and colatitude $\psi_0$. The colatitude is calculated as $\psi_0 = \arccos\hat{\boldsymbol{d}}_{z_i}(t+\Delta t)$.

The azimuth angle is:

$$\alpha_0 = \begin{cases} 0, & \text{if } \psi_0 = 0 \text{ or } \pi \\ \text{atan2}(\hat{\boldsymbol{d}}_{y_i}(t+\Delta t), \hat{\boldsymbol{d}}_{x_i}(t+\Delta t)), & \text{otherwise} \end{cases}$$

atan2 is an implementation of $\arctan(\frac{Y}{X})$ that correctly identifies the quadrant of interest.

Finally, we apply the transformation:

$$\begin{bmatrix} \hat{d}'_{x_i}(t+\Delta t)) \\ \hat{d}'_{y_i}(t+\Delta t)) \\ \hat{d}'_{z_i}(t+\Delta t)) \end{bmatrix} = \begin{bmatrix} \cos\psi_o\cos\alpha_0 & -\sin\alpha_0 & \sin\psi_0\cos\alpha_0 \\ \cos\psi_o\sin\alpha_0 & \cos\alpha_0 & \sin\psi_0\sin\alpha_0 \\ -\sin\psi_0 & 0 & \cos\psi_0 \end{bmatrix} \begin{bmatrix} \tilde{x} \\ \tilde{y} \\ \tilde{z} \end{bmatrix}$$

Thus, the intended direction with noise applied is $\hat{\boldsymbol{d}}'_i(t+\Delta t) = \hat{d}'_{x_i}(t+\Delta t))\boldsymbol{i} + \hat{d}'_{y_i}(t+\Delta t))\boldsymbol{j} + \hat{d}'_{z_i}(t+\Delta t))\boldsymbol{k}$

#### *Limiting turn angle*

After calculating the intended direction based on interactions and applying noise, we then compare this direction to the current direction and limit the turning angle accordingly.

First we find the angle between the intended direction (with noise) $\hat{\boldsymbol{d}}'_i(t+\Delta t)$ and the current velocity $\hat{\boldsymbol{v}}_i(t)$.

$$\beta_i(t+\Delta t) = \arccos\left(\hat{\boldsymbol{v}}_i(t)\cdot\hat{\boldsymbol{d}}'_i(t+\Delta t)\right)$$

If $\beta_i(t+\Delta t) \leq \theta_{\Delta t}$ then the turn limit has not been exceeded and so we set $\hat{\boldsymbol{v}}_i(t+\Delta t) = \hat{\boldsymbol{d}}'_i(t+\Delta t)$. Otherwise, we rotate the current velocity $\hat{\boldsymbol{v}}_i(t)$ by the turning limit towards the intended noisy direction $\hat{\boldsymbol{d}}'_i(t+\Delta t)$. This is implemented as follows:

1. First calculate the component of $\hat{\boldsymbol{d}}'_i(t+\Delta t)$ which is perpendicular to $\hat{\boldsymbol{v}}_i(t)$.

$$\boldsymbol{a}_i(t+\Delta t) = \hat{\boldsymbol{d}}'_i(t+\Delta t) - (\hat{\boldsymbol{v}}_i(t))(\hat{\boldsymbol{v}}_i(t)\cdot\hat{\boldsymbol{d}}'_i(t+\Delta t))$$

2. Normalise $\boldsymbol{a}_i(t+\Delta t)$

$$\hat{\boldsymbol{a}}_i(t+\Delta t) = \frac{\boldsymbol{a}_i(t+\Delta t)}{|\boldsymbol{a}_i(t+\Delta t)|}$$

3. Calculate the new direction

$$\hat{\boldsymbol{v}}_i(t+\Delta t) = \hat{\boldsymbol{v}}_i(t)\cos\theta_{\Delta t} + \hat{\boldsymbol{a}}_i(t+\Delta t)\sin\theta_{\Delta t}$$

#### *Position Updates*

After $\hat{\boldsymbol{v}}_i(t+\Delta t)$ has been calculated for each $i \in \{1, 2, ..., N\}$, the position of each bird is updated:

$$\boldsymbol{c}_i(t+\Delta t) = \boldsymbol{c}_i(t) + s\Delta t\hat{\boldsymbol{v}}_i(t+\Delta t)$$

#### *Pseudocode*

```
boids ← initialiseBoids()
env ← initialiseEnvironment() (1)
for t in range(0,max_time) do
    initialise velocity_update_store
    for boid in boids do
        Get distances to other boids
        if There are boids within the repulsion zone then
            Calculate repulsion effect and normalise
            Add noise to intended direction
            Limit turning angle
            Append velocity to velocity_update_store
```

```
        else
            Get boids in orientation zone
            if There are boids within the orientation zone then
                Calculate orientation effect and normalise
            end if
            Get boids in attraction zone
            if There are boids within attraction zone then
                Calculate attraction effect and normalise
            end if
            if orientation effect is non-zero then
                if attraction effect is non-zero then
                    Take average of these two effects and normalise
                    Add noise
                    Limit turning angle
                    Append velocity to velocity_update_store
                else
                    Add noise to orientation effect
                    Limit turning angle
                    Append velocity to velocity_update_store
                end if
            else if attraction effect is non-zero then
                Add noise to attraction effect
                Limit turning angle
                Append velocity to velocity_update_store
            else
                No interactions, hence add noise to current velocity
                Append velocity to velocity_update_store
            end if
        end if
    end for
    Update boid velocities
    Update boid positions
    Increment environment time
end for
```

### *Test 1*

The first test is the 3D analogue of the simple simulations performed by Ballerini et al[10], designed as a minimal model to compare metric and topological distance rules in response to a predator attack. Their model does not use repulsion or attraction forces (solely alignment), therefore in both the metric and topological versions of my model I set the repulsion and attraction range to 0. Having no attraction interactions leads to highly ordered parallel motion, which is not wholly representative of natural bird flocks. This point will be addressed in later tests and is not a detriment here as we use this test simply as an indicator for relative robustness of the two mechanisms. Lack of repulsion in this case is also not a large concern either as highly parallel flocks rarely produce collisions. Differences to highlight between this implementation and Ballerini et al[10] are the inclusion of the blind zone, limited turning angle, and a slightly different application of predator force. Upon investigating the model of Ballerini et al[10] and the original Self-propelled particle model from Vicsek[16], I noticed what appears to be a mathematical oversight. Implementing the original model by Vicsek[16] appears to result in incorrect movement as a result of quadrant information being lost by the tan function. Using the arctan2 function instead produces the correct motion. The only other discussion of this I could find was in[18]. This model contains the correction.

The test involves the perturbation of a highly parallel and cohesive flock. The flock is initialised with random positions within a sphere of radius 1. The boids are set in parallel motion, each having a velocity heading along the x-axis. A predator is placed in the path of the flock with an offset from the group centre of $d$. The predator applies a repulsive force to any boid within its range $r_{pred}$ - this force takes precedence over orientation forces; a boid will ignore orientation interactions if in range of the predator.

Parameters were set to represent as close a match as possible to Ballerini et al[10]. Metric and topological interaction ranges were increased to match the empirical interaction range of 6-7 birds. Topological range was set to 6, and metric range was set to 0.33 - a value which produced an average of approximately 6-7 interactions when moving in parallel flocks. Full parameter

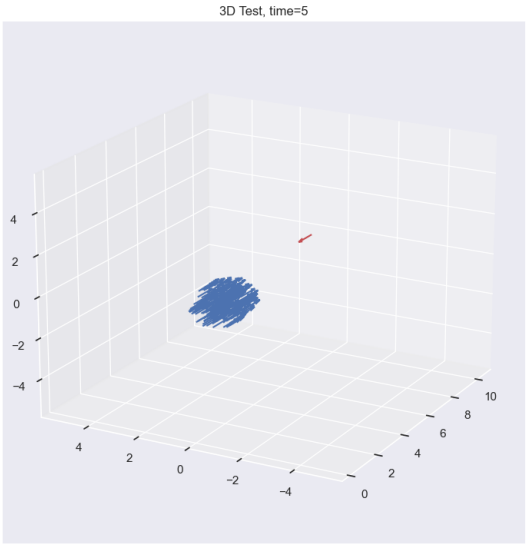


**Figure 3.** Typical setup of test 1 and 2 before the predator attack. The flock of birds is initialised with aligned velocities and random positions within a sphere. The predator (depicted as the red arrow in front of the flock) is placed in the path of the flock with a horizontal offset of d from the flock's centre.

list is shown in Table 1.

| Parameter | Value |
|---|---|
| Number of boids | 200 |
| Starting position radius | 1 |
| $d$, predator offset distance | 0.9 |
| $r_{pred}$, predator range | 1 |
| $s$, speed | 3 |
| $\Delta t$, time step interval | 0.1 |
| $\theta_{\Delta t}$, turn limit | 4° |
| $\eta$, noise standard deviation | 0 |
| $\omega_{blind}$, blind zone | 60° |
| $n_o$, topological orientation count | 6 |
| $r_o$, metric orientation range | 0.33 |
| Time steps | 1000 |

**Table 1.** Parameterisation for test 1

***Test 2***

The second test uses the same experimental setup as test 1, however this time the focus is on investigating interaction mechanisms for optimal anti-predatory flocking. Specifically, we focus on the optimal number of nearest neighbours that each bird interacts with - the optimal being the value which results in the lowest number of connected components. Here I solely focus on the topological model, and so vary $n_o$ through a range of 1-20. Ballerini et al[10] suggest that their finding of each bird interacting with 6-7 nearest neighbours could be related to the anti-predatory optimum number of interactions - this is evolutionarily viable as flocks with sub optimal interactions would likely have a higher mortality rate.

The general trend is predicted as follows: poor results for low values of $n_o$ as the information is too localised and fails to pick up on easily accessible information (the predator is likely to be close by the time information reaches a bird), poor results for high values of $n_o$ due to averaging over a large number of individuals which are likely uninformed - hence reducing the

impact of informed movement by informed individuals. Therefore, a medium value of $n_o$ is predicted to produce best results. The actual value of which is likely dependant on the model. The parameters are the same as in Table 1, except the time step is limited to 500 to reduce computational time (Qualitative trends can still be discovered within this time period, extending the time steps much further likely only leads to general dispersion over the infinite space).

#### *Test 3*

Previous tests have only used orientation forces as a means for group cohesion, test 3 introduces repulsion and attraction. The addition of the attraction term induces features such as birds on the outside of the flock moving towards the centre - an evolutionarily advantageous behaviour seen in many animals[19]. Bird velocities under these conditions are no longer perfectly parallel and so the probability of flocks splitting is non-zero. This test investigates the cohesion of the metric and topological models in an environment free from external perturbations. I introduce noise into the movement of birds by setting *eta* to 0.1. Flocks must be cohesive both with and without the presence of a predator and so I analyse the tendency of each model to produce splits in flocks, as well as the likelihood that the flock will reform.

I also test and compare a new model which combines metric and topological distances. In this model birds have both a metric and topological orientation range. This means that they will orient with the $n_o$ nearest birds within $r_o$ metric distance. This is introduced to test the idea that birds orient with those close to them and are attracted to those further away - the topological only model fails to deal with this as it orients with the nearest birds even if they are far away.

Parameters are the same as Table 1 apart from: max time steps set to 500, number of boids is 100, and tests are run with $n_o$, $n_a$, $r_o$, and $r_a$ varying over a range of suitable values.

## Results

#### *Metric vs Topological interactions for robust cohesion under external perturbations*

The simple setup of test 1 provided results consistent with the simulations of Ballerini et al[10]. The flock with topological interactions maintained greater cohesion than the metric model. This is seen in the average number of connected components (CCs) after the attack, visualised in Figure 4. Taking time step 500 as a point of comparison, the topological model had on average 5.25 CCs, compared to 8.1 CCs for the metric model. Due to the lack of attraction, the number of connected components is likely an overestimate as boids expand into the infinite environment. For comparison with Ballerini et al[10] I plot the distribution of the number of CCs for each model in Figure 5.

By analysing visual representations of the model we can gain insight into typical behaviour - Figure 6 shows the distribution of birds after the attack for a run of the metric and the topological model. In the topological model all birds are travelling in relatively the same direction. This indicates that with normal attractive forces seen in nature this flock would be likely to maintain cohesion - the predator would have a hard time separating individuals from the collective. Many metric runs produce distributions that involve one or more birds heading in significantly differing directions to the flock. This change of heading, and crucially the lack of fast corrective action, gives the predator greater chance of catching its prey. Figure 7 shows the fast corrective action of the topological model.

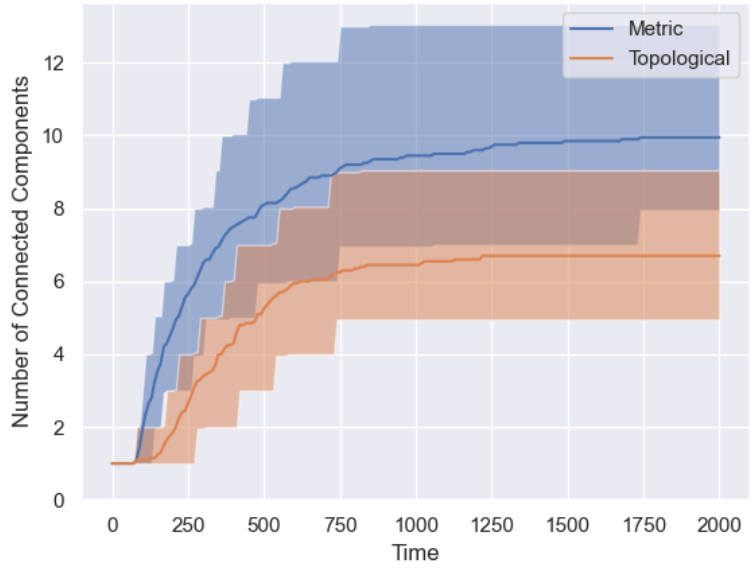


**Figure 4.** Average number of connected components (CCs) over time for both the metric and topological models - with 5th and 95th percentile range at each time point. The is calculated from a set of 20 runs each. The topological model maintains a significantly lower number of CCs in the majority of runs.

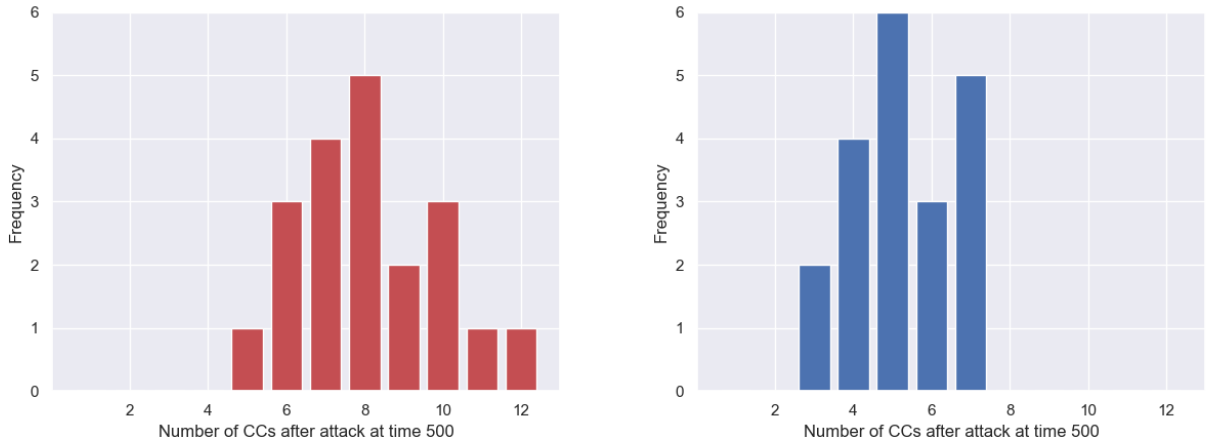


**Figure 5.** Distribution of connected components over 20 runs each of the metric (left) and topological (right) models. Results are not as clear as the two dimensional case in Ballerini et al[10], neither model manages to maintain a single cohesive flock. This is largely due to the larger degrees of freedom in the three-dimensional case, making cohesion harder to maintain. Although not as clear cut, the topological model still produces a lower number of CCs in general.

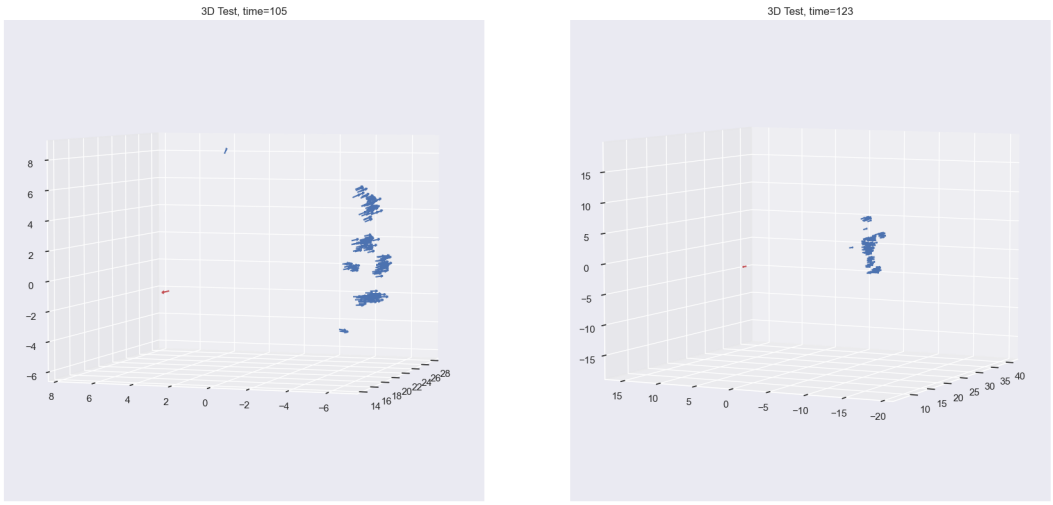


**Figure 6.** Typical formation of birds after attack in test 1: left) metric interactions, right) topological interactions. The metric model often results in solo birds or small groups of birds being separated from the group and heading to the left of the predator - this increases their risk of predation due to separation. The topological model maintains a much tighter shape and typically does not result in small groups being separated far from the main flock.

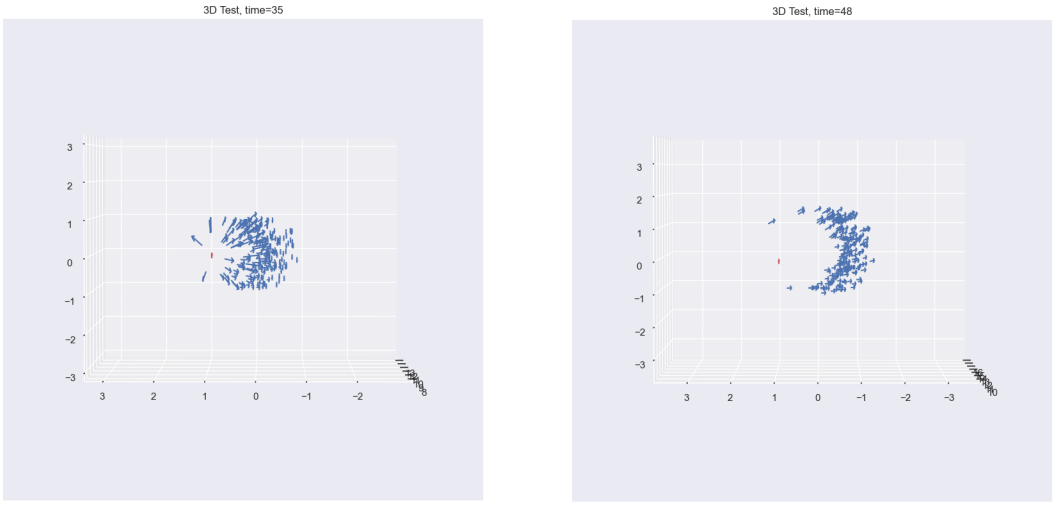


**Figure 7.** A predator attack on the topological model. Left: Birds that have detected the predator react and change heading to escape. Right: Birds that had to break cohesion with the flock to escape quickly correct their heading and move back towards the flock. A metric model encountering the attack displayed in the left image would likely not see this corrective action, and birds would remain separated from the group.

***Anti-predatory optimum number of interactions***

Data from test 2 did not provide support for the hypothesis of low and high values of $n_o$ responding worse than an optimum middle value to predators. Analysis of the number of connected components after attack resulted in increasing cohesion as $n_o$ increased - tested values were $n_o \in \{1,3,5,7,9,11,19\}$. Analysis of the number of birds entering a "capture zone" (Chosen to be a quarter of $r_{pred}$) which we associate with the prey being caught by the predator did not highlight significant differences when $n_o$ was varied.

The seeming lack of coherent and meaningful insight gained from this test is likely a result of an unsuitable testing environment and/or poorly chosen parameters. Hence, I do not propose that these results should be taken as evidence supporting an alternative hypothesis, but instead I highlight the need for careful experimental design - especially regarding the challenge of modelling biological collective behaviour.

***Long-term behaviour of Metric vs topological interactions in flocks free from external perturbation***

Analysis of flocks moving undisturbed and freely in space shows that topological only interactions do not produce greater long-term cohesion: seen in Figure 8. Parameters tested were chosen within an approximated biologically plausible range for the topological model, with the number of nearest neighbour interactions being 6-7. This is harder to estimate for the metric model and so tests were run to find parameters that resulted in interactions with again approximately 6-7 birds. Neither model consistently maintains a single cohesive flock, this is a known problem in both the topological and metric models - they require a large number of interactions (larger than biologically plausible) to produce cohesive flocks.

An alternative model which does produce cohesive flocks with a suitable number of interactions is one that combines metric and topological distances - as described earlier in test 3. As seen in Figure 9 this model's long-term behaviour is the maintenance of a single cohesive flock in the majority of cases. An initial decrease in cohesion takes place due to the random starting positions, however the model is able to recover and unite the separated flocks. Within the tests performed, a greater number of orientation interactions leads to faster recovery of cohesion.

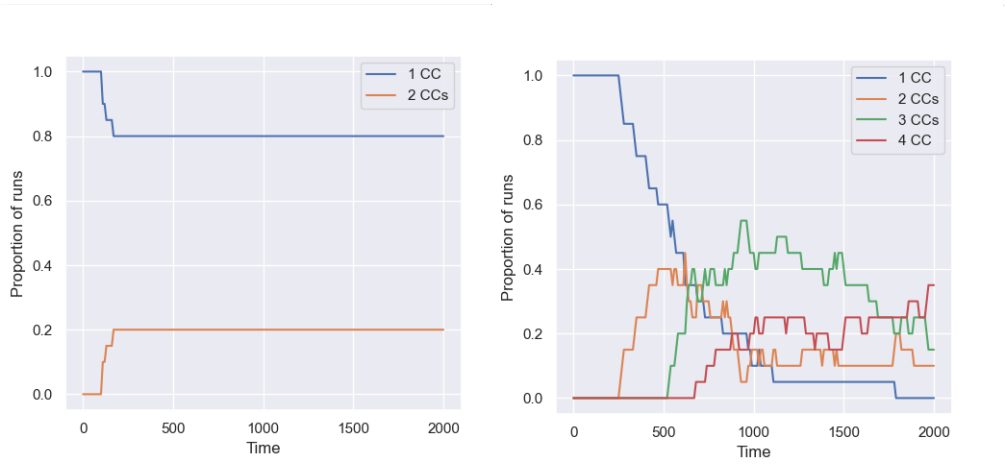


**Figure 8.** Average number of connected components over 20 runs against time: left) Metric model with $r_o = 5$ and $r_a = 10$ right) Topological model with $n_o = 5$ and $n_a = 1$. Neither model manages to consistently maintain a single cohesive flock. However, at these parameters the topological only model performs much worse than the metric only model. It must be noted that this particular comparison should not be taken as evidence of better cohesion in metric models as the metric model has significantly higher numbers of interacting individuals. Both models increase in cohesion as number of interactions increase.

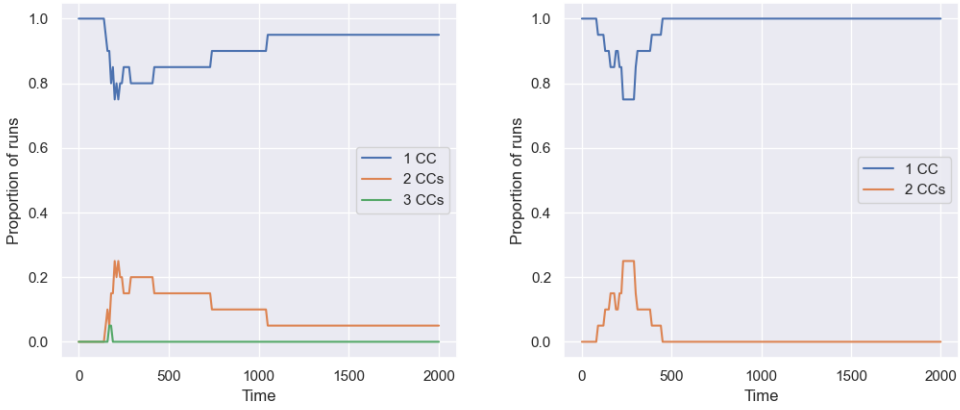


**Figure 9.** Average number of connected components over 20 runs against time for combined metric and topological model: left) $n_o = 3$ and $n_a = 1$ right) $n_o = 5$ and $n_a = 1$. Flocks initially display non-cohesive behaviour due to the random starting position. Most runs recover cohesion within the group and settle into dynamic parallel motion as a united flock. The simulations with the higher number of orientation interactions per bird displayed faster recovery of cohesion. This model can produce cohesive flocks with a biologically plausible number of interactions.

## Discussion

The primary aim of this report was to extend the work of Ballerini et al[10] and to test the hypothesis that topological interaction mechanisms produce more cohesive flocks under external perturbations than metric mechanisms. Through the analysis of the minimal setup in test 1 I have produced evidence which tentatively supports this hypothesis. A flock using topological distances tends to result in fewer connected components than one using metric distances. The simplification of movement that was used in this test does provoke questions as to the legitimacy of this claim with regard to bird flocks. Stronger evidence would be produced by analysing a model which had dynamic parallel movement and the ability for birds to be attracted to one another - rather than simply aligning. By not including the ability to attract - and therefore the ability to combine separated flocks - we are missing a crucial part of the process of robust cohesion. Another element which should be considered with robust cohesion is the likelihood of predation for a model. In experimental setup 1 this could be thought of as the number of birds that enter a range close to the predator. A flock could remain completely cohesive by simply not reacting to the predator, but this would not be advantageous in terms of survivability. Hence, it would be sensible to test for a mechanism that offers the optimum balance of predator avoidance and quick recovery time.

Ballerini et al[10] suggested that a possible reason for birds interacting with 6 to 7 nearest neighbours could be a result of this being the anti-predatory optimum. The tests performed in this report relating to this hypothesis (test 2) were found to not be adequate to capture relevant data. Further testing of this hypothesis would likely benefit from more extensive testing of model parameters and features. Upon re-evaluation the choice of predator range may not have been sensible. Ballerini et al[10] use a force which is applied to each bird and decays proportionally to the reciprocal of the distance to the predator. I chose to apply a uniform force on all birds within a set metric range of the predator. The reasoning for this was so that only birds near the front of the flock - and therefore those with greatest vision of the predator - would react to and adjust their direction. The intention was that birds behind those at the front (those less likely to see the predator) would adjust their heading based on the birds around them, and not knowledge of a predator they may not have seen, as in the model by Ballerini et al[10]. In practice, the small metric predator range and the uniform repulsive force within this meant that birds did not react in a very natural manner to the predator. A possible alternative for further work would be to apply a repulsive force probabilistically to birds. Where the repulsive force increases as distance decreases, and birds further back in the flock have lower chance of being repulsed - simulating their decreased likelihood of seeing the predator. This could also be handled by introducing blocking bodies for birds - meaning that a bird would not detect a predator if its line of view was blocked by another bird.

The comparison between metric and topological models is hindered by their poor cohesion for realistic numbers of interactions. As noted in[12], flocks are likely to split unless each bird interacts with roughly 10-15% of other birds in these models. The introduction and testing of the combined metric and topological model in this report provides an interesting solution to this problem, and further investigation into the plausibility of this model would be valuable.

The simplicity of many previous models has been useful for the general study of flocking, however if we wish to understand the methods of organisms such as the Starling, the design and testing of more biologically plausible models will also be crucial. Works such as Hildenbrandt et al[17] set an example of modelling whilst taking into account natural features and constraints. They use a model where all movement of birds is a result of their local interactions with an approximately fixed number of neighbours. This is a vast improvement on previous models that would use global information such as attraction to the centre of the flock - a calculation that is not viable due to cognitive limitations[20].

The work of this report may have been overambitious in its aims due to underestimation of the complexity of producing and analysing a three-dimensional biologically motivated model. The additional degrees of freedom introduced coupled with an unbounded environment mean that models need to be well analysed before they can be used to test hypothesis. Even so, the tests performed, as well as the encountered problems, in this report will be a useful guide for further work.

## References


1. Batchelder, D. Starlings at brighton pier. (2023).
2. Doran, C. e. a. Fish waves as emergent collective antipredator behavior. *Curr. Biol.* **32**, 708–714, DOI: https://doi.org/10.1016/j.cub.2021.11.068 (2022).
3. Parrish, V. S. V., J. K. & Grunbaum, D. Self-organized fish schools: an examination of emergent properties. *The biological bulletin* **202**, 296–305, DOI: https://doi.org/10.2307/1543482 (2002).
4. Schaller, V. e. a. Polar patterns of driven filaments. *Nature* **467**, 73–77, DOI: https://doi.org/10.1038/nature09312 (2010).
5. Peron, T. D. M. & Rodrigues, F. A. Collective behavior in financial markets. *Europhys. Lett.* **96**, DOI: https://doi.org/10.1209/0295-5075/96/48004 (2011).
6. Sugiyama, Y. e. a. Traffic jams without bottlenecks—experimental evidence for the physical mechanism of the formation of a jam. *New journal physics* **10**, DOI: https://doi.org/10.1088/1367-2630/10/3/033001 (2008).

7. Powell, G. V. N. Experimental analysis of the social value of flocking by starlings (sturnus vulgaris) in relation to predation and foraging. *Animal Behav.* **22**, 501–505, DOI: https://doi.org/10.1016/S0003-3472(74)80049-7 (1974).

8. Thompson, W. A., Vertinsky, I. & Krebs, J. R. The survival value of flocking in birds: A simulation model. *J. Animal Ecol.* **43**, 785–820, DOI: https://doi.org/10.2307/3537 (1974).

9. Reynolds, C. W. Flocks, herds and schools: A distributed behavioral model. *Proc. 14th annual conference on Comput. graphics interactive techniques* 25–34, DOI: https://doi.org/10.1145/37401.37406 (1987).

10. Ballerini, M. e. a. Interaction ruling animal collective behavior depends on topological rather than metric distance: Evidence from a field study. *Proc. national academy sciences* **105**, 1232–1237, DOI: https://doi.org/10.1073/pnas.0711437105 (2008).

11. Couzin, I. D. e. a. Collective memory and spatial sorting in animal groups. *J. theoretical biology* **218**, 1–11, DOI: https://doi.org/10.1006/jtbi.2002.3065 (2002).

12. Mudaliar, R. K. e. a. Systematic analysis of emergent collective motion produced by a 3d hybrid zonal model. *Bull. mathematical biology* **84**, 1–25, DOI: https://doi.org/10.1007/s11538-021-00977-2 (2022).

13. Chakraborty, B. S., D. & De, R. Survival chances of a prey swarm: how the cooperative interaction range affects the outcome. *Sci. Reports* **10**, 1–8, DOI: https://doi.org/10.1038/s41598-020-64084-3 (2020).

14. Grégoire, C. H., G. & Tu, Y. Moving and staying together without a leader. *Phys. D: Nonlinear Phenom.* **181**, 157–170, DOI: https://doi.org/10.1016/S0167-2789(03)00102-7 (2003).

15. Bode, F. D. W., N. W. & Wood, A. J. Limited interactions in flocks: relating model simulations to empirical data. *J. The Royal Soc. Interface* **8**, 301–304, DOI: https://doi.org/10.1098/rsif.2010.0397 (2011).

16. Vicsek, T. e. a. Novel type of phase transition in a system of self-driven particles. *Phys. review letters* **75**, 1226, DOI: https://doi.org/10.1103/PhysRevLett.75.1226 (1995).

17. Hildenbrandt, C. C. H. C. K., H. Self-organized aerial displays of thousands of starlings: a model. *Behav. Ecol.* **21**, 1349–1359, DOI: https://doi.org/10.1093/beheco/arq149 (2010).

18. Chen, G. Small noise may diversify collective motion in vicsek model. *Transactions on Autom. Control.* **62**, 636–651, DOI: https://doi.org/10.1109/TAC.2016.2560144 (2016).

19. Vine, I. Risk of visual detection and pursuit by a predator and the selective advantage of flocking behaviour. *J. Theor. Biol.* **30**, 405–422, DOI: https://doi.org/10.1016/0022-5193(71)90061-0 (1971).

20. Emmerton, J. & Delius, J. D. Beyond sensation: visual cognition in pigeons. 377–399 (1993).